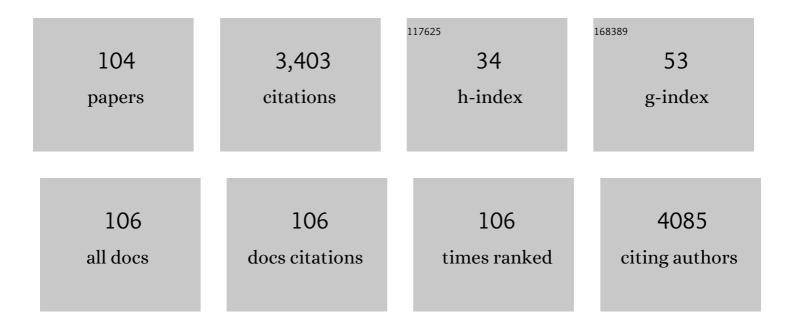
List of Publications by Year in descending order

Source: https://exaly.com/author-pdf/2133363/publications.pdf Version: 2024-02-01



LONCZHEN OUL

#	Article	IF	CITATIONS
1	Construction of Builtâ€In Electric Field within Silver Phosphate Photocatalyst for Enhanced Removal of Recalcitrant Organic Pollutants. Advanced Functional Materials, 2020, 30, 2002918.	14.9	133
2	Responses of microalgae Coelastrella sp. to stress of cupric ions in treatment of anaerobically digested swine wastewater. Bioresource Technology, 2018, 251, 274-279.	9.6	114
3	Effects of copper ions on removal of nutrients from swine wastewater and on release of dissolved organic matter in duckweed systems. Water Research, 2019, 158, 171-181.	11.3	108
4	Sustainable livestock wastewater treatment via phytoremediation: Current status and future perspectives. Bioresource Technology, 2020, 315, 123809.	9.6	104
5	Highly selective and sensitive sensor based on an organic electrochemical transistor for the detection of ascorbic acid. Biosensors and Bioelectronics, 2018, 100, 235-241.	10.1	103
6	Fabrication of Aligned Nanofiber Polymer Yarn Networks for Anisotropic Soft Tissue Scaffolds. ACS Applied Materials & Interfaces, 2016, 8, 16950-16960.	8.0	102
7	Synthesis of 0D Manganeseâ€Based Organic–Inorganic Hybrid Perovskite and Its Application in Leadâ€Free Red Lightâ€Emitting Diode. Advanced Functional Materials, 2021, 31, 2100855.	14.9	98
8	An ABA triblock copolymer strategy for intrinsically stretchable semiconductors. Journal of Materials Chemistry C, 2015, 3, 3599-3606.	5.5	93
9	Insights into mechanisms of UV/ferrate oxidation for degradation of phenolic pollutants: Role of superoxide radicals. Chemosphere, 2020, 244, 125490.	8.2	88
10	Efficient degradation of tetracycline by singlet oxygen-dominated peroxymonosulfate activation with magnetic nitrogen-doped porous carbon. Journal of Environmental Sciences, 2022, 115, 330-340.	6.1	85
11	Living nano-micro fibrous woven fabric/hydrogel composite scaffolds for heart valve engineering. Acta Biomaterialia, 2017, 51, 89-100.	8.3	81
12	Effective Use of Electrically Insulating Units in Organic Semiconductor Thin Films for Highâ€Performance Organic Transistors. Advanced Electronic Materials, 2017, 3, 1600240.	5.1	80
13	Microalgal and duckweed based constructed wetlands for swine wastewater treatment: A review. Bioresource Technology, 2020, 318, 123858.	9.6	74
14	Chirality detection of amino acid enantiomers by organic electrochemical transistor. Biosensors and Bioelectronics, 2018, 105, 121-128.	10.1	73
15	A bis(2-oxoindolin-3-ylidene)-benzodifuran-dione containing copolymer for high-mobility ambipolar transistors. Chemical Communications, 2014, 50, 3180.	4.1	72
16	Enhanced activation of peroxymonosulfte by LaFeO3 perovskite supported on Al2O3 for degradation of organic pollutants. Chemosphere, 2019, 237, 124478.	8.2	72
17	Polymer blends with semiconducting nanowires for organic electronics. Journal of Materials Chemistry, 2012, 22, 4244.	6.7	66
18	Enhanced near-infrared photoresponse of organic phototransistors based on single-component donor–acceptor conjugated polymer nanowires. Nanoscale, 2016, 8, 7738-7748.	5.6	65

#	Article	IF	CITATIONS
19	Organic Field-Effect Transistors with Macroporous Semiconductor Films as High-Performance Humidity Sensors. ACS Applied Materials & Interfaces, 2017, 9, 14974-14982.	8.0	62
20	Adsorptive removal of anionic dye using calcined oyster shells: isotherms, kinetics, and thermodynamics. Environmental Science and Pollution Research, 2019, 26, 5944-5954.	5.3	62
21	Self-stratified semiconductor/dielectric polymer blends: vertical phase separation for facile fabrication of organic transistors. Journal of Materials Chemistry C, 2013, 1, 3989.	5.5	59
22	Incorporation of Heteroatoms in Conjugated Polymers Backbone toward Air-Stable, High-Performance <i>n</i> -Channel Unencapsulated Polymer Transistors. Chemistry of Materials, 2018, 30, 5451-5459.	6.7	55
23	Electrically switchable photoluminescence of fluorescent-molecule-dispersed liquid crystals prepared via photoisomerization-induced phase separation. Journal of Materials Chemistry C, 2014, 2, 1386.	5.5	52
24	Enhanced Strategies for Antibiotic Removal from Swine Wastewater in Anaerobic Digestion. Trends in Biotechnology, 2021, 39, 8-11.	9.3	51
25	Bar-Coated Ultrathin Semiconductors from Polymer Blend for One-Step Organic Field-Effect Transistors. ACS Applied Materials & Interfaces, 2018, 10, 21510-21517.	8.0	50
26	Solutionâ€Processed Microporous Semiconductor Films for Highâ€Performance Chemical Sensors. Advanced Materials Interfaces, 2016, 3, 1600518.	3.7	47
27	A luminescent liquid crystal with multistimuli tunable emission colors based on different molecular packing structures. New Journal of Chemistry, 2014, 38, 3429.	2.8	44
28	Preparation, Performances, and Mechanisms of Microbial Flocculants for Wastewater Treatment. International Journal of Environmental Research and Public Health, 2020, 17, 1360.	2.6	44
29	Fast and deep oxidative desulfurization of dibenzothiophene with catalysts of MoO ₃ –TiO ₂ @MCM-22 featuring adjustable Lewis and BrÃ,nsted acid sites. Catalysis Science and Technology, 2019, 9, 6166-6179.	4.1	43
30	Performance and biofilm characteristics of biotrickling filters for ethylbenzene removal in the presence of saponins. Environmental Science and Pollution Research, 2018, 25, 30021-30030.	5.3	42
31	Circularly Polarized Photodetectors Based on Chiral Materials: A Review. Frontiers in Chemistry, 2021, 9, 711488.	3.6	42
32	Effect of presence of hydrophilic volatile organic compounds on removal of hydrophobic n-hexane in biotrickling filters. Chemosphere, 2020, 252, 126490.	8.2	42
33	Facile green synthesis of isoindigo-based conjugated polymers using aldol polycondensation. Polymer Chemistry, 2017, 8, 3448-3456.	3.9	38
34	Piezoelectric Poly(vinylidene fluoride) (PVDF) Polymer-Based Sensor for Wrist Motion Signal Detection. Applied Sciences (Switzerland), 2018, 8, 836.	2.5	37
35	A new thieno-isoindigo derivative-based D–A polymer with very low bandgap for high-performance ambipolar organic thin-film transistors. Polymer Chemistry, 2015, 6, 3970-3978.	3.9	36
36	Improved Transistor Performance of Isoindigo-Based Conjugated Polymers by Chemically Blending Strongly Electron-Deficient Units with Low Content To Optimize Crystal Structure. Macromolecules, 2018, 51, 370-378.	4.8	36

#	Article	IF	CITATIONS
37	Fused Heptacyclic-Based Acceptor–Donor–Acceptor Small Molecules: N-Substitution toward High-Performance Solution-Processable Field-Effect Transistors. Chemistry of Materials, 2019, 31, 2027-2035.	6.7	33
38	Sb ₂ S ₃ solar cells: functional layer preparation and device performance. Inorganic Chemistry Frontiers, 2019, 6, 3381-3397.	6.0	33
39	Bis(2-oxoindolin-3-ylidene)-benzodifuran-dione-based D–A polymers for high-performance n-channel transistors. Polymer Chemistry, 2015, 6, 2531-2540.	3.9	32
40	A Fast Response Ammonia Sensor Based on Coaxial PPy–PAN Nanofiber Yarn. Nanomaterials, 2016, 6, 121.	4.1	32
41	Sequential vertical flow trickling filter and horizontal flow multi-soil-layering reactor for treatment of decentralized domestic wastewater with sodium dodecyl benzene sulfonate. Bioresource Technology, 2020, 300, 122634.	9.6	31
42	Helical Nanofibrils of Block Copolymer for High-Performance Ammonia Sensors. ACS Applied Materials & Interfaces, 2018, 10, 22504-22512.	8.0	30
43	Organic thin-film transistors with a photo-patternable semiconducting polymer blend. Journal of Materials Chemistry, 2011, 21, 15637.	6.7	29
44	Photocatalytic performances of heterojunction catalysts of silver phosphate modified by PANI and Cr-doped SrTiO3 for organic pollutant removal from high salinity wastewater. Journal of Colloid and Interface Science, 2020, 561, 379-395.	9.4	27
45	Intrinsically Stretchable <i>n</i> -Type Polymer Semiconductors through Side Chain Engineering. Macromolecules, 2021, 54, 8849-8859.	4.8	27
46	Phototransistors based on a donor–acceptor conjugated polymer with a high response speed. Journal of Materials Chemistry C, 2015, 3, 10734-10741.	5.5	26
47	Flexible and low-voltage organic phototransistors. RSC Advances, 2017, 7, 11572-11577.	3.6	23
48	Modulating charge transport characteristics of bis-azaisoindigo-based D–A conjugated polymers through energy level regulation and side chain optimization. Journal of Materials Chemistry C, 2019, 7, 7618-7626.	5.5	23
49	Side-Chain Engineering To Optimize the Charge Transport Properties of Isoindigo-Based Random Terpolymers for High-Performance Organic Field-Effect Transistors. Macromolecules, 2019, 52, 4765-4775.	4.8	23
50	Enabling discrimination capability in an achiral F6BT-based organic semiconductor transistor <i>via</i> circularly polarized light induction. Journal of Materials Chemistry C, 2020, 8, 9271-9275.	5.5	22
51	High-efficiency self-healing conductive composites from HPAMAM and CNTs. Journal of Materials Chemistry A, 2015, 3, 12154-12158.	10.3	21
52	Induction of circularly polarized electroluminescence from achiral poly(fluorene- <i>alt</i> -benzothiadiazole) by circularly polarized light. Journal of Materials Chemistry C, 2020, 8, 6521-6527.	5.5	20
53	Deep Blue Layered Lead Perovskite Lightâ€Emitting Diode. Advanced Optical Materials, 2021, 9, 2001709.	7.3	20
54	Deep Ultraviolet Light Stimulated Synaptic Transistors Based on Poly(3-hexylthiophene) Ultrathin Films. ACS Applied Materials & Interfaces, 2022, 14, 11718-11726.	8.0	19

#	Article	IF	CITATIONS
55	Cholesteric liquid crystals with an electrically controllable reflection bandwidth based on ionic polymer networks and chiral ions. Journal of Materials Chemistry C, 2015, 3, 5406-5411.	5.5	18
56	Modulating the Surface via Polymer Brush for Highâ€Performance Inkjetâ€Printed Organic Thinâ€Film Transistors. Advanced Electronic Materials, 2017, 3, 1600402.	5.1	18
57	Air-Stable and High-Performance Unipolar n-Type Conjugated Semiconducting Polymers Prepared by a "Strong Acceptor–Weak Donor―Strategy. ACS Applied Materials & Interfaces, 2020, 12, 17790-1779	98 ^{8.0}	18
58	Taming Charge Transport and Mechanical Properties of Conjugated Polymers with Linear Siloxane Side Chains. Macromolecules, 2021, 54, 5440-5450.	4.8	18
59	Low-temperature melt processed polymer blend for organic thin-film transistors. Journal of Materials Chemistry, 2012, 22, 18887.	6.7	17
60	Bis(2-oxo-7-azaindolin-3-ylidene)benzodifuran-dione-based donor–acceptor polymers for high-performance n-type field-effect transistors. Polymer Chemistry, 2017, 8, 2381-2389.	3.9	17
61	Light-Emitting Diodes with Manganese Halide Tetrahedron Embedded in Anti-Perovskites. ACS Energy Letters, 2021, 6, 1901-1911.	17.4	17
62	Side Chain Engineering: Achieving Stretch-Induced Molecular Orientation and Enhanced Mobility in Polymer Semiconductors. Chemistry of Materials, 2022, 34, 2696-2707.	6.7	17
63	Thickness dependence of the electro-optical properties of reverse-mode polymer-stabilised cholesteric texture. Liquid Crystals, 2014, 41, 1382-1387.	2.2	16
64	Nanofiber-structured hydrogel yarns with pH-response capacity and cardiomyocyte-drivability for bio-microactuator application. Acta Biomaterialia, 2017, 60, 144-153.	8.3	16
65	Rational molecular design for isoindigo-based polymer semiconductors with high ductility and high electrical performance. Journal of Materials Chemistry C, 2019, 7, 11639-11649.	5.5	16
66	Benzotrithiophene and benzodithiophene-based polymers for efficient polymer solar cells with high open-circuit voltage. Polymer Chemistry, 2013, 4, 3390.	3.9	15
67	A phthalimide- and diketopyrrolopyrrole-based A ₁ –π–A ₂ conjugated polymer for high-performance organic thin-film transistors. Polymer Chemistry, 2015, 6, 418-425.	3.9	15
68	Bis(2-oxoindolin-3-ylidene)-benzodifuran-dione and bithiophene-based conjugated polymers for high performance ambipolar organic thin-film transistors: the impact of substitution positions on bithiophene units. Journal of Materials Chemistry C, 2016, 4, 6391-6400.	5.5	15
69	Tuning helical twisting power and photoisomerisation kinetics of axially chiral cyclic azobenzene dopants in cholesteric liquid crystals. Liquid Crystals, 2019, 46, 2181-2189.	2.2	15
70	Azaisoindigo-Based Polymers with a Linear Hybrid Siloxane-Based Side Chain for High-Performance Semiconductors Processable with Nonchlorinated Solvents. ACS Applied Materials & Interfaces, 2020, 12, 41832-41841.	8.0	14
71	Preparation and characterization of microporous sodium poly(aspartic acid) nanofibrous hydrogel. Journal of Porous Materials, 2017, 24, 75-84.	2.6	13
72	High-contrast electrically switchable light-emitting liquid crystal displays based on α-cyanostilbenic derivative. Liquid Crystals, 2018, 45, 32-39.	2.2	12

#	Article	IF	CITATIONS
73	High-efficiency synthesis of a naphthalene-diimide-based conjugated polymer using continuous flow technology for organic field-effect transistors. Journal of Materials Chemistry C, 2019, 7, 8450-8456.	5.5	12
74	Highly Sensitive Polymer Phototransistor Based on the Synergistic Effect of Chemical and Physical Blending in D (Donor)–A (Acceptor) Copolymers. Advanced Electronic Materials, 2019, 5, 1900174.	5.1	12
75	Characterisation and effect of polymer network deformation in reverse-mode polymer-stabilised cholesteric texture. Liquid Crystals, 2017, 44, 437-443.	2.2	11
76	One-pot synthesized ABA tri-block copolymers for high-performance organic field-effect transistors. Polymer Chemistry, 2018, 9, 4517-4522.	3.9	11
77	Band-edge-enhanced tunable random laser using a polymer-stabilised cholesteric liquid crystal. Liquid Crystals, 2021, 48, 255-262.	2.2	11
78	Ultrathin Polythiophene Films Prepared by Vertical Phase Separation for Highly Stretchable Organic Fieldâ€Effect Transistors. Advanced Electronic Materials, 2021, 7, 2100591.	5.1	11
79	Submillisecond-Response Light Shutter for Solid-State Volumetric 3D Display Based on Polymer-Stabilized Cholesteric Texture. Journal of Display Technology, 2014, 10, 396-401.	1.2	10
80	Polymer-stabilised cholesteric liquid-crystals as tunable light-reflector with low operating-voltage and energy consumption. Liquid Crystals, 2020, 47, 1655-1662.	2.2	9
81	Tri-state switching of a high-order parameter, double-layered guest-host liquid-crystal shutter, doped with the mesogenic molecule 4HPB. Liquid Crystals, 2021, 48, 1555-1561.	2.2	9
82	Cell gap effects on domain size and electro-optical properties of normal-mode polymer-stabilised cholesteric texture. Liquid Crystals, 2015, 42, 255-260.	2.2	8
83	Regulation and control of polymer network deformation in reverse-mode polymer-stabilised cholesteric texture. Liquid Crystals, 2017, 44, 688-694.	2.2	8
84	Aza-Based Donor-Acceptor Conjugated Polymer Nanoparticles for Near-Infrared Modulated Photothermal Conversion. Frontiers in Chemistry, 2019, 7, 359.	3.6	7
85	Physical properties of liquid crystals doped with CsPbBr ₃ quantum dots. Liquid Crystals, 2021, 48, 1357-1364.	2.2	7
86	Continuously tunable emission color based on the molecular aggregation of (2Z,2′Z)-2,2′-(1,4-phenylenae)bis(3-(4-(dodecyloxy)phenyl)acrylonitrile). RSC Advances, 2016, 6, 96196-96	20 ³ 1.	6
87	Highly polarized absorption and emission from polymer-stabilized smectic guest-host systems. Liquid Crystals, 2019, 46, 1574-1583.	2.2	6
88	Asymmetric Hybrid Siloxane Side Chains for Enhanced Mobility and Mechanical Properties of Diketopyrrolopyrroleâ€Based Polymers. Macromolecular Rapid Communications, 2022, 43, e2100636.	3.9	6
89	Electrically controllable reflection bandwidth polymer-stabilized cholesteric liquid crystals with low operating voltage. Liquid Crystals, 2022, 49, 1314-1321.	2.2	5
90	Au-Induced Directional Growth of Inkjet-Printed 6,13-Bis(triisopropylsilylethynyl) Pentacene. Journal of Display Technology, 2015, 11, 450-455.	1.2	4

#	Article	IF	CITATIONS
91	FePc induced highly oriented PIID-BT conjugated polymer semiconductor with high bias-stress stability. Applied Physics Letters, 2018, 113, .	3.3	4
92	Performance and Biomass Characteristics of SBRs Treating High-Salinity Wastewater at Presence of Anionic Surfactants. International Journal of Environmental Research and Public Health, 2020, 17, 2689.	2.6	4
93	Solutionâ€Processed Ultrathin Semiconductor Films for Highâ€Performance Ammonia Sensors. Advanced Materials Interfaces, 2021, 8, 2100493.	3.7	4
94	Purification and characterization of anti-phytopathogenic fungi angucyclinone from soil-derived Streptomyces cellulosae. Folia Microbiologica, 2022, 67, 517-522.	2.3	4
95	Role of Molecular Weight in the Mechanical Properties and Charge Transport of Conjugated Polymers Containing Siloxane Side Chains. Macromolecular Rapid Communications, 2022, , 2200149.	3.9	4
96	Influence of Curing Frequency on the Morphology and the Electro-Optical Property of Polymer-Stabilized Cholesteric Textures. Molecular Crystals and Liquid Crystals, 2014, 588, 9-16.	0.9	3
97	Liquid Crystal Polarisation Converter Arrays Based on Microholes Patterned Hydrophobic Layers. Liquid Crystals, 2021, 48, 1873-1879.	2.2	3
98	Inkjet Printed Poly(3-hexylthiophene) Thin-Film Transistors: Effect of Self-Assembled Monolayer. Molecular Crystals and Liquid Crystals, 2014, 593, 201-213.	0.9	2
99	The effect of MWS polarisation on the morphology and electro-optical behaviour of normal-mode polymer-stabilised cholesteric textures. Liquid Crystals, 2016, 43, 540-546.	2.2	2